#6166

NEW WALL FUNCTIONS FOR THE NUMERICAL SIMULATION OF AIR FLOW PATTERN IN ROOMS

X. Yuan, A. Huber, A. Schaelin, P. Hachmann, and A. Moser
Energy Systems Laboratory
Swiss Federal Institute of Technology Zurich
CH-8092 Zurich, Switzerland

SUMMARY

Numerical simulation of air flow patterns in rooms has made considerable progress in recent years. However, for real applications in rooms, an important problem remains the accurate prediction of heat flux at the walls. Due to grid resolution, wall functions have to be used for the correct representation of the boundary conditions. Improved wall functions allow a better trade-off between reasonable computing time and accuracy, in particular for 3-dimensional calculations.

New wall functions in conjunction with a low-Reynolds-number k-ε model are proposed to improve the calculation results. New wall functions are developed for velocity, temperature, turbulent kinetic energy, and dissipation rate of turbulent kinetic energy. It is shown that they are valid for a wide range of wall distances.

The model is applied to flat plate cases and to an air-filled closed cavity case. The comparison of numerical results with experimental data indicates that the new wall functions can improve the prediction of air flows in the cases considered, and at the same time, save expensive grid lines.

NOMENCLATURE

Symbol	Meaning	Unit
A^+	a constant in Equation 1	[-]
B^+	a constant in Equation 1	[-]
h	specific enthalpy of fluid	[J/kg]
h_s	specific enthalpy of fluid which is immediately adjacent to the wall	[J/kg]
K	mixing length constant for momentum	[-]
K'	mixing length constant for heat	[-]
k	turbulent kinetic energy	[J/kg]
k^+	dimensionless turbulent kinetic energy k/u_τ^2	[-]
L	length of the plate	[m]
p	pressure	[Pa]
Pr_l	molecular Prandtl number	[-]
Pr_t	turbulent Prandtl number	[-]
q_s	wall heat flux	[W/m^2]
Re	Reynolds number U_0L/υ	[-]
Re_x	x-Reynolds number U_0x/υ	[-]
St	Stanton number $q_s/(\rho c_p U_0(T_s-T_0))$	[-]
T_0	temperature of free stream	[^{0}C]
T_s	temperature of the plate surface	[^{0}C]
T^+	dimensionless temperature $\rho u_\tau(h_s - h)/q_s$	[-]
u	mean velocity component in the streamwise direction	[m/s]
u_τ	friction velocity $(\tau_s/\rho)^{0.5}$	[-]
u^+	dimensionless streamwise velocity u/u_τ	[-]
U_0	mean velocity of free stream	[m/s]
v	mean velocity component normal to the wall	[m/s]
x	distance in the streamwise direction	[m]
y	distance normal to the wall	[m]
y_n	distance from wall to the nodal point of near-wall mesh	[mm]
y^+	local Reynolds number yu_τ/υ	[-]
y^+_n	local Reynolds number of near-wall grid $y_n u_\tau/\upsilon$	[-]
ε	turbulence dissipation rate	[J/kg·s]
ε^+	dimensionless turbulence dissipation rate $\upsilon\varepsilon/u_\tau^4$	[-]
μ	molecular viscosity	[N·s/m^2]
μ_{eff}	effective viscosity $\mu + \mu_t$	[N·s/m^2]
μ_t	turbulent viscosity	[N·s/m^2]
μ^+	dimensionless effective viscosity μ_{eff}/μ	[-]
υ	kinematic viscosity	[m^2/s]
ρ	density of fluid	[kg/m^3]
σ_{eff}	effective Prandtl number $\mu_{eff}/\sigma_{eff} = \mu/Pr_l + \mu_t/Pr_t$	[-]
τ_s	wall shear stress	[Pa]

NEW WALL FUNCTIONS FOR THE NUMERICAL SIMULATION OF AIR FLOW PATTERN IN ROOMS

X. Yuan, A. Huber, A. Schaelin, P. Hachmann, and A. Moser

Energy Systems Laboratory
Swiss Federal Institute of Technology Zurich
CH-8092 Zurich, Switzerland

INTRODUCTION

Numerical simulation of air flow patterns within buildings has made considerable progress in recent years. The computational fluid dynamics (CFD) techniques may be used to predict air velocity, temperature, and contaminant concentration distributions as reviewed by several researchers [1, 2]. However, for real applications, an important problem remains the accurate prediction of heat flux at the walls, since heat transfer is not only related to the room air mean and wall temperatures but also to the local temperature and velocity profiles.

The boundary layer on the walls in rooms is turbulent and the heat transfer is by natural convection (or forced convection when the supply inlet is close to the wall). As there are no appropriate wall functions for natural convection when the standard k-ε turbulence model is applied to room air flows, forced convection wall functions, or traditional wall functions are normally employed. As a result, the predicted heat transfer is very sensitive to the computational grid spacing near the wall. The coarse grid gives too-low convective heat transfer and vice-versa, as reported by Chen [3] and Li [4]. That means that the standard k-ε model in conjunction with the traditional wall functions can not predict the wall heat flux in room air flows.

Low-Reynolds-number k-ε turbulence models are considered to be able to predict wall heat flux in natural convection, since the models are also valid in the near wall region, hence the wall functions are not necessary. However, at least 10 grid lines [5], or even 20 to 30 [2] are required in the near-wall region, which significantly increases the computing cost, and limits a practical wide applicability of the models.

Is there any approach to predict wall heat flux without too much computing cost? To study one such approach is the aim of this paper.

Figure 1 shows velocity and temperature profiles near a heated wall. The typical value of the distance from the wall to the position of maximum velocity is about 5 mm and the local Reynolds number, y^+, is less than 20 for room air flows. Choosing a mesh system with the nodal point of the first cell near the maximum velocity position will not cause too much computing cost, and will also be expected in order to obtain sufficient information from the result of CFD. But appropriate wall functions are then necessary.

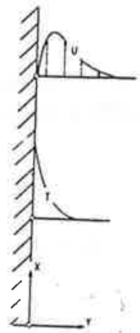

Figure 1 Velocity and temperature profile near a heated wall

NEW WALL FUNCTIONS

New wall functions for velocity, temperature, turbulent kinetic energy, and dissipation rate are developed in this section. Because of the complexity of natural convection, the new wall functions were deduced on the basis of forced convection, but a variable turbulent Prandtl number is applied and much attention was paid in the low local Reynolds number region.

Turbulent Prandtl Number

Turbulent Prandtl number, Pr_t, is defined as the ratio of the eddy diffusivity of momentum to that of enthalpy.

The research on turbulent Prandtl number is very active and a great number of publications are available [6-22]. The behavior of turbulent Prandtl number is complex, it depends on the type of flow (wall flow, core flow, or free flow), molecular Prandtl number, Reynolds number (or Rayleigh number for natural convection) and position. Figure 2 and Table 1 show the curves of Pr_t versus y^+ and their conditions. It is obvious from Fig. 2 that Pr_t levels off within a band from 0.7 to 1.0 when $y^+ > 120$. Therefore a constant Pr_t is a reasonable choice in numerical simulation of room air flows in this region. When $y^+ < 40$, Pr_t values in Fig. 2 vary in a large range. Since the value of y^+ of the near-wall node in numerical simulation of room air flows is normally less than 40, the variation of turbulent Prandtl number should be taken into account.

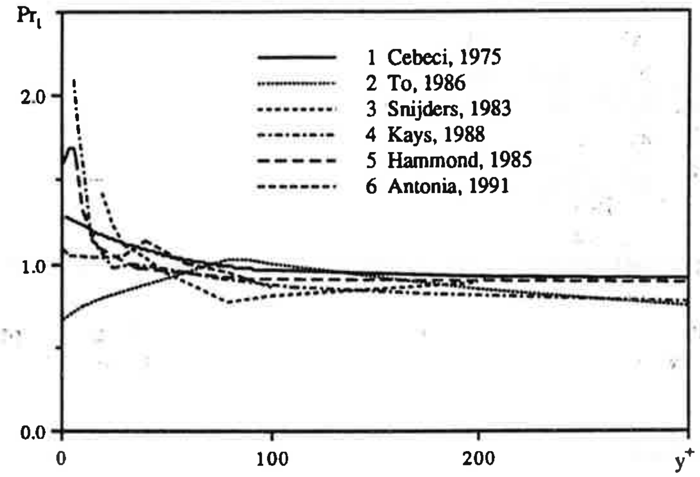

Figure 2 Turbulent Prandtl number functions

Table 1 Details of the Pr_t functions presented in Fig. 2

Curve	Author and year	Approach	Flow type
1	Cebeci, 1975	analysis	forced and natural, flat plate
2	To, 1986	calculation	natural, heated vertical flat plate
3	Snijders, 1983	measurement	mixed, heated flat plate
4	Kays, 1988	measurement	forced, flat plate
5	Hammond, 1985	analysis	based on log-law wall function
6	Antonia, 1991	calculation	forced, channel flow

In the present study, we adopt the suggestion of Cebeci [8]. He proposed that turbulent Prandtl number is a function of y^+, i.e.,

$$Pr_t = \frac{K(1-\exp(-y^+/A^+))}{K'(1-\exp(-y^+/B^+))} \tag{1}$$

where K, K', A^+, and B^+ are constants. Their values are given below Eq. 8.

The New Wall Functions for Velocity and Temperature

For a two-dimensional boundary layer, under the assumption that the variation of u, h, and ρ with x can be neglected (couette flow), the Reynolds equation can be expressed by:

$$\rho v \frac{\partial u}{\partial y} = \frac{\partial}{\partial y}\left(\mu_{eff}\frac{\partial u}{\partial y}\right) - \frac{\partial p}{\partial x} \tag{2}$$

$$\rho v \frac{\partial h}{\partial y} = \frac{\partial}{\partial y}\left(\frac{\mu_{eff}}{\sigma_{eff}}\frac{\partial h}{\partial y}\right) \tag{3}$$

in terms of Reynolds-averaged variables. It follows from mass continuity that $\rho v = 0$. When

$$\frac{\partial p}{\partial x} = 0$$

Eqs. 2 and 3 become

$$\frac{du^+}{dy^+} = \frac{1}{\mu^+} \tag{4}$$

$$\frac{dT^+}{dy^+} = \frac{\sigma_{eff}}{\mu^+} \tag{5}$$

If the van-Driest's hypothesis [23] for μ_t,

$$\mu^+ = 1 + K^2 {y^+}^2 (1 - \exp(-y^+/A^+))^2 \frac{du^+}{dy^+} \tag{6}$$

is used and substituting Eq. 1 into Eqs. 4 and 5, we obtain

$$\frac{du^+}{dy^+} = \frac{2}{1 + \{1 + 4K^2 {y^+}^2 [1 - \exp(-y^+/A^+)]^2\}^{0.5}} \tag{7}$$

$$\frac{dT^+}{dy^+} = \left(\frac{1}{Pr_l} + \frac{2KK' {y^+}^2 [1 - \exp(-y^+/A^+)][1 - \exp(-y^+/B^+)]}{1 + \{1 + 4K^2 {y^+}^2 [1 - \exp(-y^+/A^+)]^2\}^{0.5}}\right)^{-1} \tag{8}$$

Supposing $K = 0.435$, $K' = K/0.9$, $A^+ = 26$, $B^+ = 37$, and $Pr_l = 0.71$, numerically integrating Eqs. 7 and 8, and then fitting curves piece-wise, we obtain the velocity and temperature distributions, i.e., the new wall functions, as follows:

$$u^+ = y^+ \quad \text{for} \quad 0 < y^+ \leq 5$$
$$u^+ = 4.82\ln y^+ - 2.75 \quad \text{for} \quad 5 < y^+ \leq 16 \qquad (9)$$
$$u^+ = 3.47\ln y^+ + 0.98 \quad \text{for} \quad 16 < y^+ \leq 42.2$$
$$u^+ = 2.32\ln y^+ + 5.27 \quad \text{for} \quad y^+ > 42.2$$

$$T^+ = Pr_l y^+ \quad \text{for} \quad 0 < y^+ \leq 5$$
$$T^+ = 4.15\ln y^+ - 3.13 \quad \text{for} \quad 5 < y^+ \leq 18.6 \qquad (10)$$
$$T^+ = 3.60\ln y^+ - 1.52 \quad \text{for} \quad 18.6 < y^+ \leq 44.5$$
$$T^+ = 2.13\ln y^+ + 4.05 \quad \text{for} \quad y^+ > 44.5$$

A similar fitting procedure was proposed by Chen [24] who connected the linear law with the traditional log-law by a logarithmic segment.

The exact curves obtained by numerical integration and the new wall functions are plotted in Figures 3 and 4. It can be seen from the figures that the fitted curves approximate the exact ones very well.

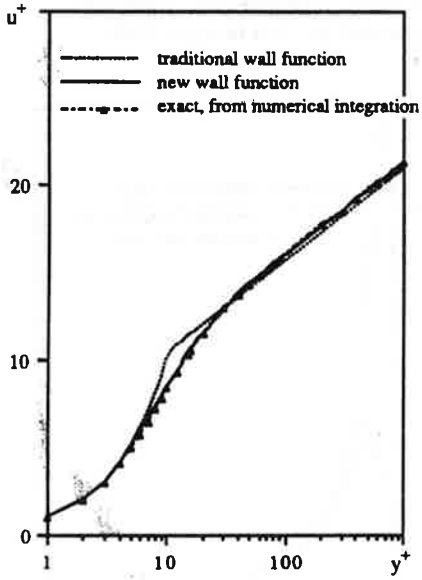

Figure 3 Wall function for velocity

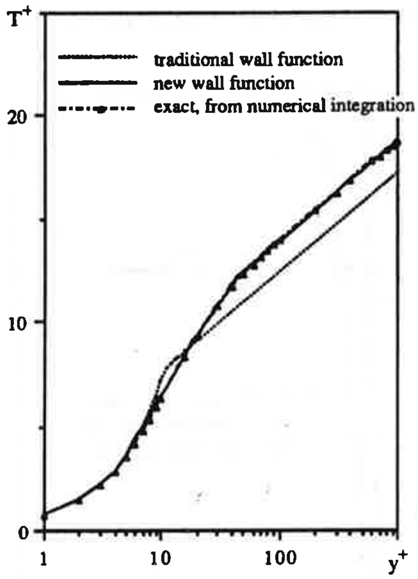

Figure 4 wall function for temperature

In order to see the difference between variable turbulent Prandtl number and constant turbulent Prandtl number, the traditional wall functions [25] are also plotted in Figures 3 and 4. The traditional ones are:

$$u^+ = \frac{1}{K}\ln(9y^+) \tag{11}$$

$$T^+ = Pr_t(u^+ + P) \tag{12}$$

$$P = \frac{\pi}{4\sin(\pi/4)}\left(\frac{A^+}{K}\right)^{\frac{1}{2}}\left(\frac{Pr_l}{Pr_t} - 1\right)\left(\frac{Pr_t}{Pr_l}\right)^{\frac{1}{4}} \tag{13}$$

The curves plotted in the figures are with $K = 0.435$, $A^+ = 26$, $Pr_t = 0.9$ and $Pr_l = 0.71$, namely,

$$u^+ = 2.30\ln y^+ + 5.05 \tag{14}$$

$$T^+ = 2.07\ln y^+ + 2.81 \tag{15}$$

The New Wall Functions for k and ε

Patel et al. (1985) [26] reviewed experimental data on the turbulent kinetic energy and dissipation rate, and presented the distributions of k and ε in the near-wall region, as shown in Figures 5 and 6. The uncertainty of the experimental data is about 30%.

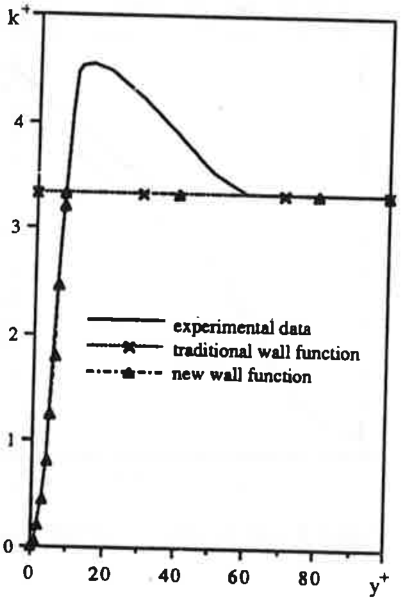

Figure 5 Wall function for turbulent kinetic energy

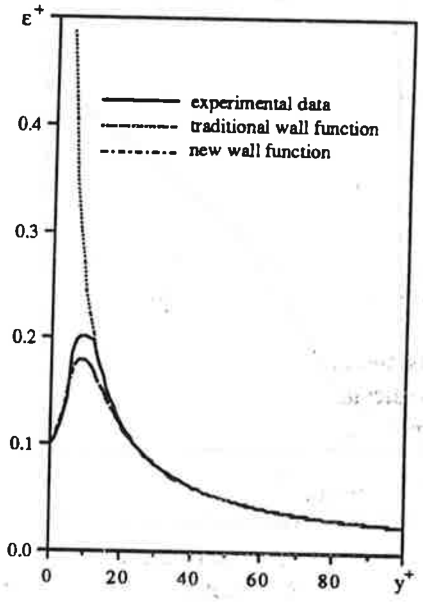

Figure 6 Wall function for dissipation rate

The traditional wall functions for k and ε are also plotted in Figures 5 and 6 from which it can be seen that the traditional wall functions are not valid in the region of $y^+ < 10$. To complement the functions in this region, the suggestion by Sirkar and Hanratty [27] for the function for k is employed and the function for ε is obtained by means of curve fit. We impose new wall functions as

$$k^+ = \min\{3.33,\ 0.05y^{+2}\} \tag{16}$$

$$\varepsilon^+ = \frac{0.1 + 0.003y^{+^2}}{1 + 0.00125y^{+^3}}\ , \tag{17}$$

They are also shown in the figures.

VALIDATION OF THE NEW WALL FUNCTIONS

In this section the results of numerical simulation based on the two kinds of wall functions -- the traditional wall functions and the new wall functions -- are compared with the experimental data of forced convection on flat plates and natural convection in a closed cavity.

Forced Convection on Flat Plates

Moffat and Kays [28] presented a heat transfer equation in terms of local Stanton number for a smooth, flat plate of uniform temperature,

$$\mathrm{St}\ \mathrm{Pr}_l^{\,0.4} = 0.0287\mathrm{Re}_x^{-0.2} \tag{18}$$

which is the best fit of the experimental data for Reynolds numbers from 2×10^5 to 3.6×10^6. Here, x is the distance from the flat plate leading edge.

The two kinds of wall functions in conjunction with the standard k-ε model are applied to calculate the turbulent boundary layer for 5 cases. The main parameters of the 5 cases are listed in Table 2.

The comparison of calculated total heat transfer between the two kinds of wall functions is presented in Figure 7. From the figure it can be seen that the calculated values based on the new wall functions are in better agreement with the experimental data in the range of $2.4\times10^5 < \mathrm{Re} < 3.6\times10^6$. Figure 8, the comparison of local heat transfer, indicates

Table 2 The main parameters of the test cases

Case	Velocity of free steam Uo [m/s]	Length of the plate L [m]	Re = LUo/υ
1	18	0.2	238,000
2	18	0.5	594,000
3	18	1.0	1,190,000
4	36	1.0	2,380,000
5	36	1.5	3,570,000
Temperature of free stream = 25 °C Temperature of the plate surface = 35 °C Width of the plate = 1 m			

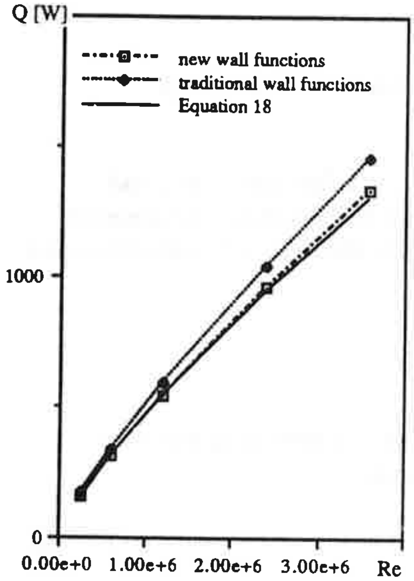

Figure 7 Comparison of total heat transfer with measurement

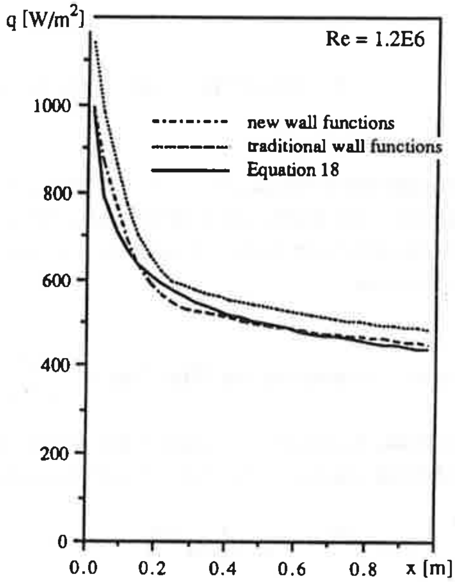

Figure 8 Comparison of local heat flux with measurement for Case 3

that the new wall functions give better results. Figure 9 shows the variation of the calculated total heat transfer of the plate, Q, with the distance of the near-wall mesh. The horizontal coordinate represents y^+_n, the distance between the wall and the first grid node near the wall in the 1/2 length of the plate. Q_m is the total heat transfer of the plate calculated from Eq. 18. Within a wide region, $45 < y^+_n < 800$, the calculated heat transfer changes less than 10 %. That means that the calculated heat transfer is almost independent of the computational grid. The same independence was found for case 1, 2, 4, and 5.

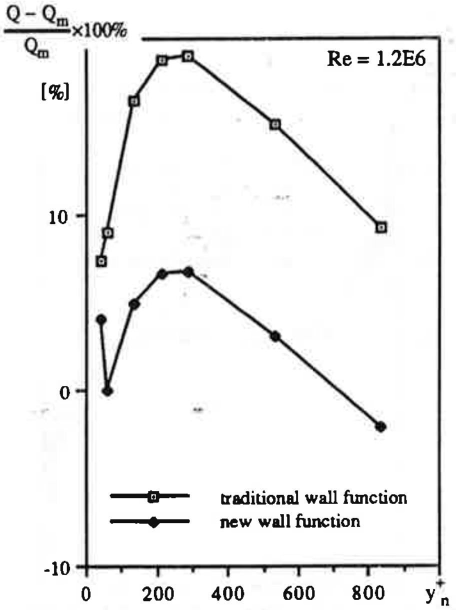

Figure 9 Variation of total heat transfer with the distance of near-wall mesh, Case 3

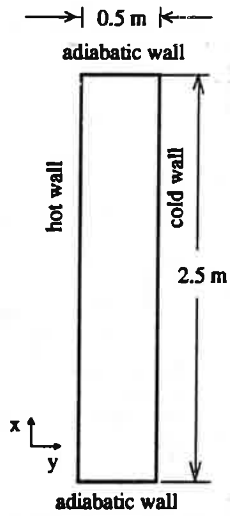

Figure 10 Sketch of the air-filled cavity, Ref. [29]

Natural Convection in a Closed Cavity

The experimental results of natural convection in a air-filled closed cavity published by Cheesewright et al. [29] are also used to validate the new wall functions. The cavity is 2.5 m high and 0.5 m wide, as shown in Figure 10. The top and bottom walls are insulated. The temperature difference between the hot and cold walls is 45.8 K.

The numerical results based on four models are compared with the experimental data: *1*: the standard k-ε model with the traditional wall functions ('St + traditional' for short in Figs. 11 to 15), *2*: the standard k-ε model with the new wall functions ('St + new'), *3*: the low-Reynolds-number model proposed by Lam and Bremhorst with the traditional wall functions ('LB + traditional'), and *4*: the low-Reynolds-number model with the new wall functions ('LB + new').

Figure 11 shows the variations of calculated total heat transfer of the cavity, Q, with the distance from wall to the nodal point of the near-wall cell, y_n. Due to heat loss from top, bottom, and side walls, the heat transfer on the cold wall, Q_c, is less than that on the hot wall, Q_h, in the experiment. If the insulation were better, Q_c would increase, and Q_h decrease since core temperature rises. The average value perhaps can be regarded as the total heat transfer. It can be seen from the figure that calculated heat transfer based on the standard k-ε model is very sensitive to y_n, while the heat transfer based on the low-

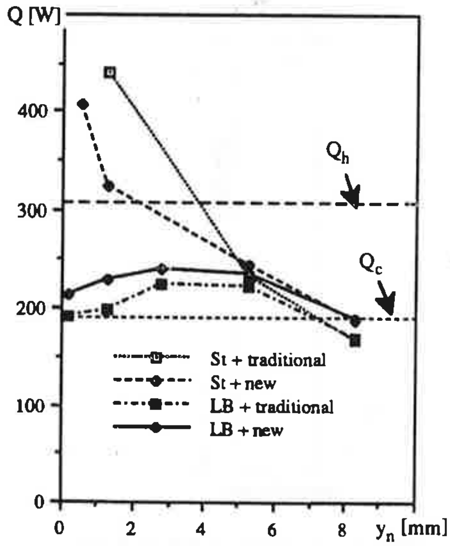

Figure 11 Variation of total heat transfer with the distance of near wall grid

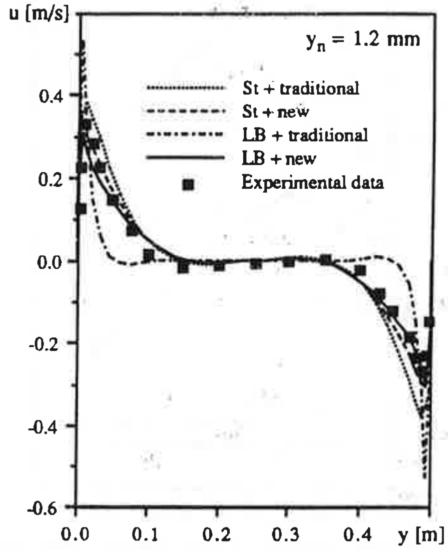

Figure 12 Profiles of vertical component of velocity at half-height

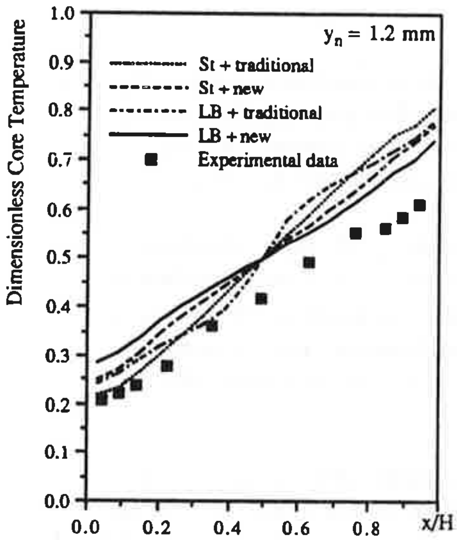

Figure 13 Vertical temperature profiles in the mid-section

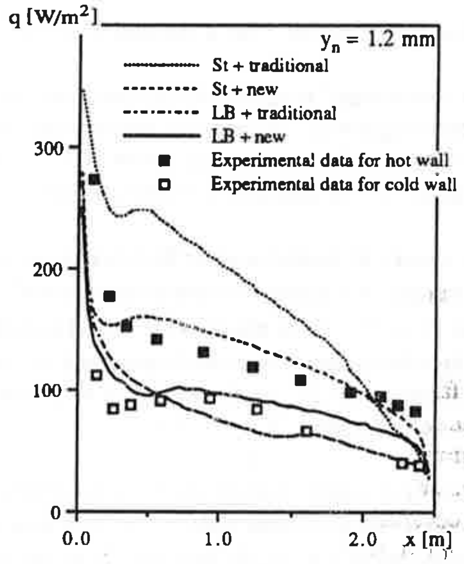

Figure 14 Profiles of local heat flux on vertical wall

Reynolds-number model changes very little in the region of $1.2 < y_n < 5.3$ mm. The low-Reynolds-number model with the new wall functions gives best results in this case. Of course, total heat transfer is not a conclusive criterion of a valid model.

The comparison of velocity profiles at half-height, Figure 12, indicates that the numerical results based on the new wall functions are close to the measured velocity profile.

Figure 13 shows the vertical temperature profiles in the mid-section. Due to imperfect insulation, the measured temperature is lower than the calculated temperature. From the point of view of the temperature gradient, the results based on the new wall functions are in better agreement with the measurements.

The local heat flux profiles are presented in Figure 14. The measured heat fluxes on both, hot and cold walls are plotted in the figure. The predicted profile located in the region between the measured heat flux on the hot and cold walls is regarded as good. It can be seen that the low-Reynolds-number model with the new wall functions gives the best result.

Figure 15 shows the turbulent kinetic energy profiles at half-height. Two peaks appear within each boundary layer in the calculated profiles with the traditional wall functions with both turbulence models. That indicates that the traditional wall function for k is not valid in the region very close to the wall.

All of the calculated results shown in Figures 12 to 15 are obtained under the condition of same mesh system in which the value of y_n is 1.2 mm. Of the four models, the low-Reynolds-number model with the new wall functions gives the best results. When y_n is increased to 5.3 mm, the calculations indicate that the results based on all four models are in good agreement with experimental data.

So far, we can conclude that the traditional wall functions are only valid in a very narrow range in natural convection boundary layer, and it is difficult to apply them to practical use. The new wall functions with the low-Reynolds-number model gives grid independent results in the region of $1.2 < y_n < 5.3$ mm in the case considered. It seems possible to predict natural convection flow without using additional grids in the near-wall region.

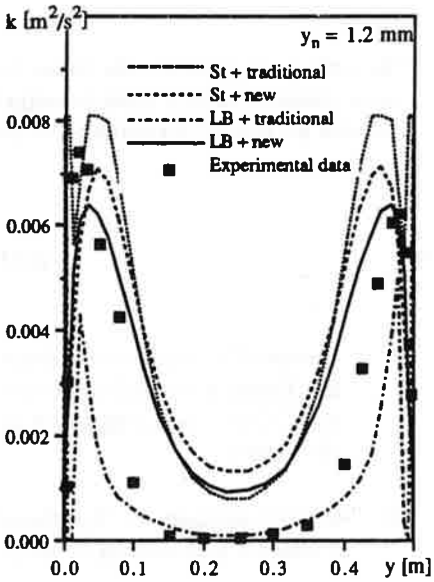

Figure 15 Profiles of turbulent kinetic energy at half-height

CONCLUSION

New wall functions for velocity, temperature, turbulent kinetic energy and turbulence dissipation rate have been proposed and implemented in a finite volume fluid dynamics code. A model for variable turbulent Prandtl numbers has been combined with an existing standard k-ε turbulence model and a low-Reynolds-number model in the near-wall region. The validations with flat plate cases and an air-filled cavity case indicate that the new wall functions can improve the numerical simulation without using additional grids in the near-wall region. In the flat plate cases, the calculated results based on the new wall functions are in better agreement with experimental data. In the cavity case, the low-Reynolds-number model with the new wall functions presents the best results of the four investigated models, and gives grid independent results for $1.2 < y_n < 5.3$ mm.

Since the wall functions are derived on the basis of forced convection, more validations are needed before the functions can be considered generally applicable to prediction of room air flows.

ACKNOWLEDGMENTS

The authors are grateful to the Swiss Federal Office of Energy (BEW) for providing partial financial support to the investigation. Particular thanks are given to Dr. Qingyan Chen for his helpful discussions and comments.

REFERENCES

[1] Nielsen P.V. "Airflow simulation techniques - progress and trends". Progress and Trends in Air Infiltration and Ventilation Research. Proceedings of the 10th AIVC Conference, Dipoli, Air Infiltration and Ventilation Center, vol 1, pp 203-223 (1989).

[2] Chen Q. and Jiang Z. "Significant questions in predicting room air motion" ASHRAE Transactions V. 98, (1992).

[3] Chen Q., Moser A., and Huber A. "Prediction of buoyant turbulent flow by a low-Reynolds-number k-ε model". ASHRAE Transactions, Vol. 96:564-573, (1990).

[4] Li Y. and Fuchs L. "An evaluation of a computer code for predicting indoor airflow and heat transfer". Air Movement and Ventilation Control within Buildings, Proceedings of 12th AIVC Conference, Ottawa, (1991).

[5] Skovgaard M., and Nielsen P.V. "Numerical investigation of transient flow over a bakward facing step using a low Reynolds number k-ε model". Air Movement and Ventilation Control within Buildings, Proceedings of 12th AIVC Conference, Ottawa, (1991).

[6] Reynolds A.J. "The prediction of turbulent Prandtl and Schmidt numbers," Int. J. Heat Mass Transfer, Vol. 18, pp. 1055-1069, (1975).

[7] Launder B.E. "Heat and mass transport". Topics in Applied Physics, Volume 12, Turbulence, ed. Bradshaw P., Springer-Verlag, (1976).

[8] Cebeci T. and Khattab A. "Prediction of turbulent-free-convective-heat transfer from a vertical flat plate". J. Heat Transfer Vol. 97, 469-471, (1975).

[9] Plumb O.A. and Kennedy L.A. "Application of a k-ε turbulence model to natural convection from a vertical isothermal surface," J. Heat Transfer, Vol. 99, PP. 79-85, (1977).

[10] Nielsen P.V., Restivo A., and Whitelaw J.H. "Buoyancy-affected flows in ventilated rooms". Numerical Heat Transfer, Vol. 2, pp. 115-127, (1979).

[11] Ideriah F.J.K. "Prediction of turbulent cavity flow driven by buoyancy and shear". J. Mech. Engng Sci., Vol. 22, PP.287-295, (1980).

[12] Snijders A.L., Koppins A.M., and Nieuwvelt C. "An experimental determination of the turbulent Prandtl number in the inner boundary layer for air flow over a flat plate". Int. J. Heat Mass Transfer, Vol. 26, PP. 425-431, (1983).

[13] Hammond G.P. "Turbulent Prandtl number within a near-wall flow". AIAA Journal, Vol. 23, pp. 1668-1669, (1985).

[14] To W.M. and Humphrey J.A.C. "Numerical simulation of buoyant, turbulent flow -- I. Free convection along a heated, vertical, flat plate". Int. J. Heat Mass Transfer, Vol. 29, pp. 573-592, (1986).

[15] Kays W.M. and Moffat R.J. "The near-wall region of the turbulent boundary layer: some results from heat transfer measurements". Near-Wall Turbulence. ed. Kline S.J. and Afgan N.H., Hemisphere, (1988).

[16] Tsuji T. and Nagano Y. "Turbulence measurements in a natural convection boundary layer along a vertical flat plate". Int. J. Heat Mass Transfer, Vol. 31, pp. 2101-2111, (1988).

[17] Kasagi N., Kuroda A., and Hirata M. "Numerical investigation of near-wall turbulent heat transfer taking into account the unsteady heat conduction in the solid wall". Journal of Heat Transfer, Vol. 111, pp. 385-392, (1989).

[18] Chua L.P. and Antonia R.A. "Turbulent Prandtl number in a circular jet," Int. J. Heat Mass Transfer, Vol. 33, pp. 331-339, (1989).

[19] Lai Y.G. and So R.M. "Near-wall modeling of turbulent heat fluxes," Int. J. Heat Mass Transfer, Vol. 33, pp. 1429-1440, (1990).

[20] Maekawa H., Kawada Y., Kobayashi M. and Yamagushi H. "An experimental study on the spanwise eddy diffusity of heat in a flat-plate turbulent boundary layer", Int. J. Heat Mass Transfer, Vol. 34, pp. 1991-1998, (1991).

[21] Antonia R. A. and Kim J. "Turbulence Prandtl number in the near-wall region of a turbulent channel flow". Int. J. Heat Mass Transfer, Vol. 34, pp. 1905-1908, (1991).

[22] Antonia R.A. and Kim J. "Reynolds shear stress and heat flux calculations in a fully developed turbulent duct flow". Int. J. Heat Mass Transfer, Vol. 34, pp. 2013-2018, (1991).

[23] van Driest E.R. "On turbulent flow near a wall". J. Aero. Sci., Vol.23, pp. 1007-1011, (1956).

[24] Chen Q. "Indoor airflow, air quality and energy consumption of buildings". PhD Thesis. Technic University of Delft, Netherlands, (1988).

[25] Patankar S.V. and Spalding D.B. "Heat and mass transfer in boundary layers". Intertext books, London, (1970).

[26] Patel V.C., Rodi W., and Scheuerer G. "Turbulence model for near-wall and low Reynolds number flows: a review". AIAA Journal, Vol. 23, pp. 1308-1319, (1985).

[27] Sirkar K.K. and Hanratty T.J. "The limiting behaviour of the turbulent transverse velocity component close to a wall". Journal of Fluid Mechanics, Vol. 44, pp. 605-614, (1970)

[28] Moffat R.J. and Kays W.M. "A review of turbulent-boundary-layer heat transfer research at Stanford, 1958-1983". Advances in Heat Transfer, Volume 16, ed. Hartnett J.P. and Irvine T.F., (1984).

[29] Cheesewright R., King K.J., and Ziai S. "Experimental data for the validation of computer code for the prediction of two-dimensional buoyant cavity flows". Significant Questions in Buoyancy Affected Enclosure or Cavity Flows. Proceedings of the Winter Annual Meeting of the ASME, California, (1986).